

**Generation of Three Dimensional Pore-Controlled Nitrogen-doped  
Graphene Hydrogels for High-Performance Supercapacitor by  
Employing Formamide as Modulator**

Yao Wang, Zidong Wei\*, Yao Nie and Yun Zhang

Chongqing Key Laboratory of Chemical Process for Clean Energy and Resource Utilization, College of Chemistry and Chemical  
Engineering.

Chongqing University, Chongqing, 400044 (China)

E-mail: zdwei@cqu.edu.cn (Wei)

## **1. Experimental section**

### **1.1. Synthesis of NGH-1, NGH -2, NGH -3, NGH -4.**

In a typical synthesis, GO aqueous suspension and formamide were mixed under vigorous stirring. After 2h vigorous stirring, the mixed solution was transferred into a Teflon-lined stainless steel autoclave, a thermal treatment was performed for the Teflon-liner in an electric oven at 180°C for 12h. By altering the volume ratio of GO aqueous suspension and formamide ( $V_{GO}: V_{formamide} = 2:8, 4:6, 6:4, 8:2$ , respectively.), four NGHs were produced, referred as to NGH-1, NGH-2, NGH-3, NGH-4, respectively. Then the obtained NGHs were freeze-dried.

### **1.2 Characterization of catalysts**

The morphology and structure of NGHs were observed under field emission scanning electron microscopy (FE-SEM, JSM-7800F (JEOL)). Low-resolution transmission electron microscopy (TEM) was carried out on a Zeiss LIBRA 200 FETEM instrument operating at 200 kV. The crystal structures of NGHs were confirmed using the automated X-ray diffraction equipment (XRD, Rigaku D/MaXIII A, Japan). The surface area of NGHs is calculated from N<sub>2</sub> adsorption isotherms using Brunauer-Emmett-Teller BET (Shimadzu, Micromeritics ASAP 2010 Instrument). XPS was acquired using a Kratos XSAM800 spectrometer equipped with monochromatic Al X-ray source (Al KR, 1.4866 keV), and the binding energy was calibrated by using 284.6 eV as the C 1s peak energy.

### **1.3. Electrochemical activity tests**

Electrochemical measurements: All electrochemical experiments were performed in a standard three-electrode cell at room temperature on a Parstat 2273 potentiostat/galvanostat workstation assembled with a model 636 rotational system (AMETEK) at room temperature. The cell is consisting of a glassy carbon working electrode (GC electrode, 5 mm in diameter, PINE: AFE3T050GC), an Ag/AgCl (saturated KCl) reference electrode, and a platinum foil counter electrode. All potentials in this study, however, are given relative to the reversible hydrogen electrode (RHE). The working electrodes were prepared by applying catalyst ink onto glassy carbon (GC) disk electrodes. In brief, the samples were dispersed in ethanol and ultrasonicated for 15 minutes to form a uniform catalyst ink. Well-dispersed sample ink was applied onto a pre-polished

GC disk. After drying at room temperature, a drop of 0.05 wt. % Nafion solution was applied onto the surface of the sample layer to form a thin protective film.

The samples were characterized by a cyclic voltammetry (CV) and galvanostatic charge–discharge cycling were performed at room temperature in 6 M aqueous KOH in the potential range 0 to 0.8 V (ORR). The scan rate for CV is 5, 10, 20, 50, 100, 200 mV/s, respectively.

Electrochemical impedance spectroscopy (EIS) measurements were carried out using an electrochemical work station (CHI660b, Chen Hua Instruments Co. Ltd. , Shanghai).

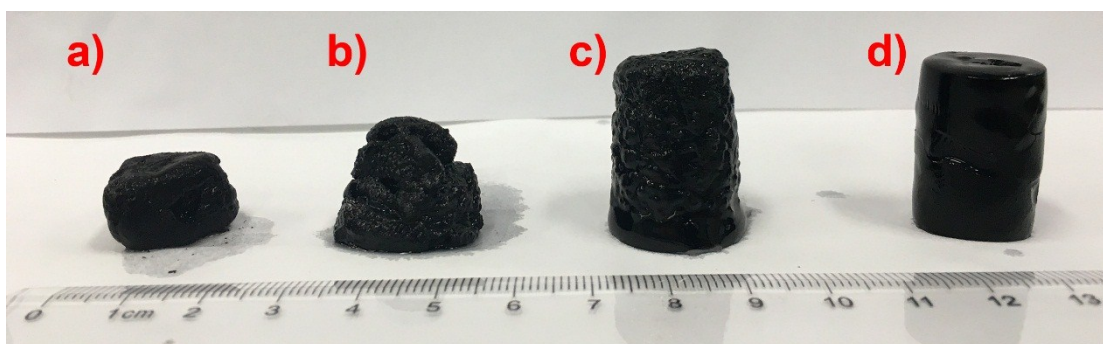


Fig. S1. Digital images of the NGHs; a). NGH-1, b). NGH-2, c). NGH-3, d). NGH-4,

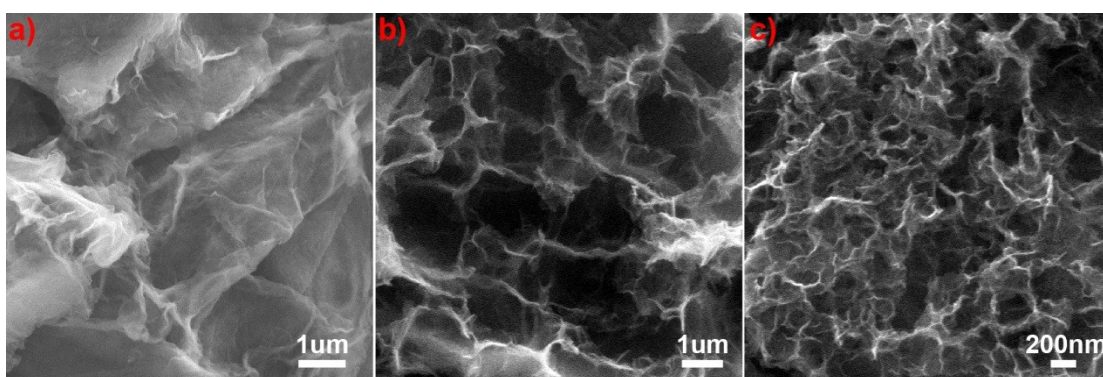


Fig. S2. SEM of graphene oxide (a) and NGH-3 (b, c)

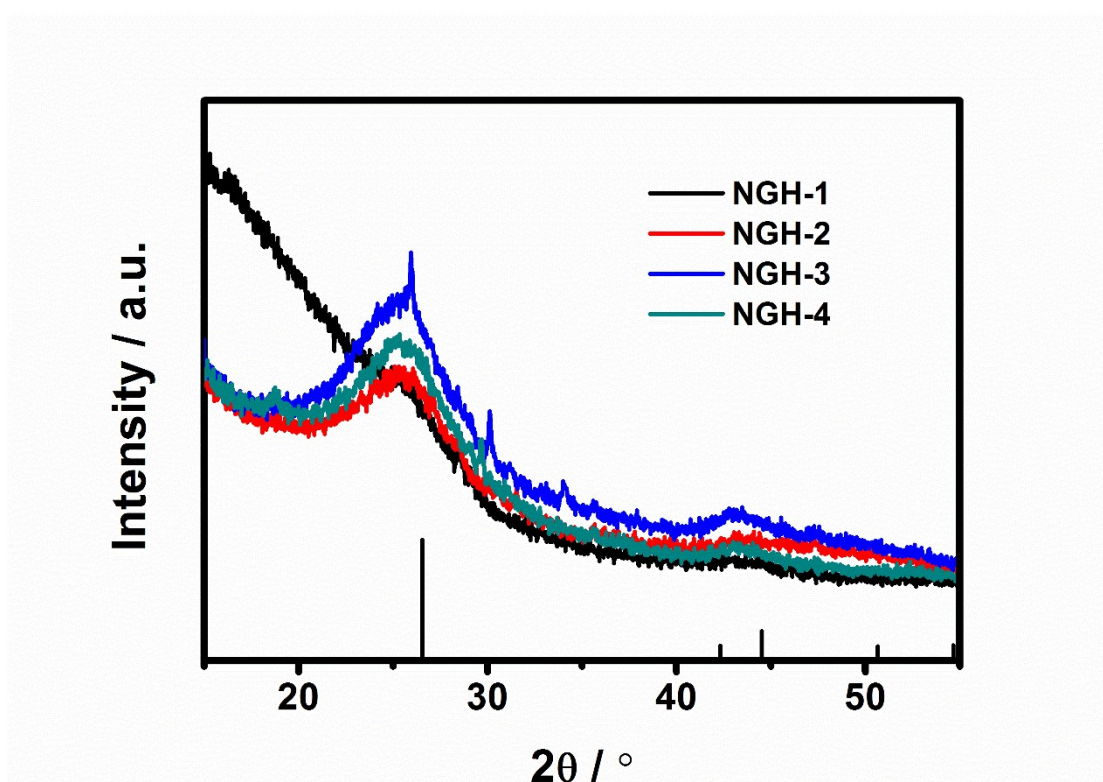


Fig. S3. XRD pattern of NGHs

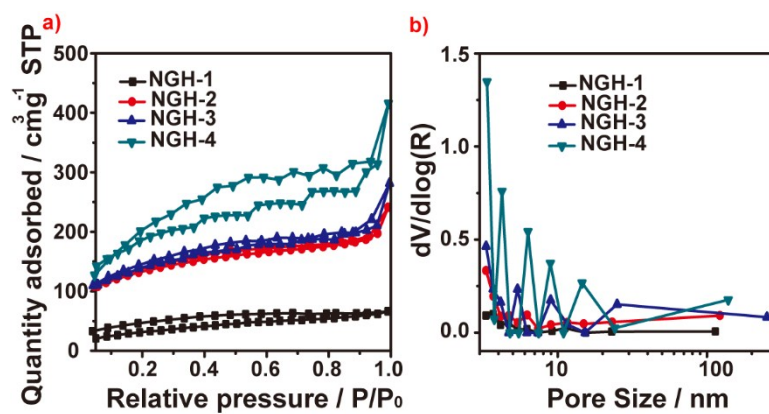


Fig. S4. (a)  $\text{N}_2$  Adsorption (black line)- desorption (red line) isotherms of various NGHs; (b) Pore size distribution curves of various NGHs

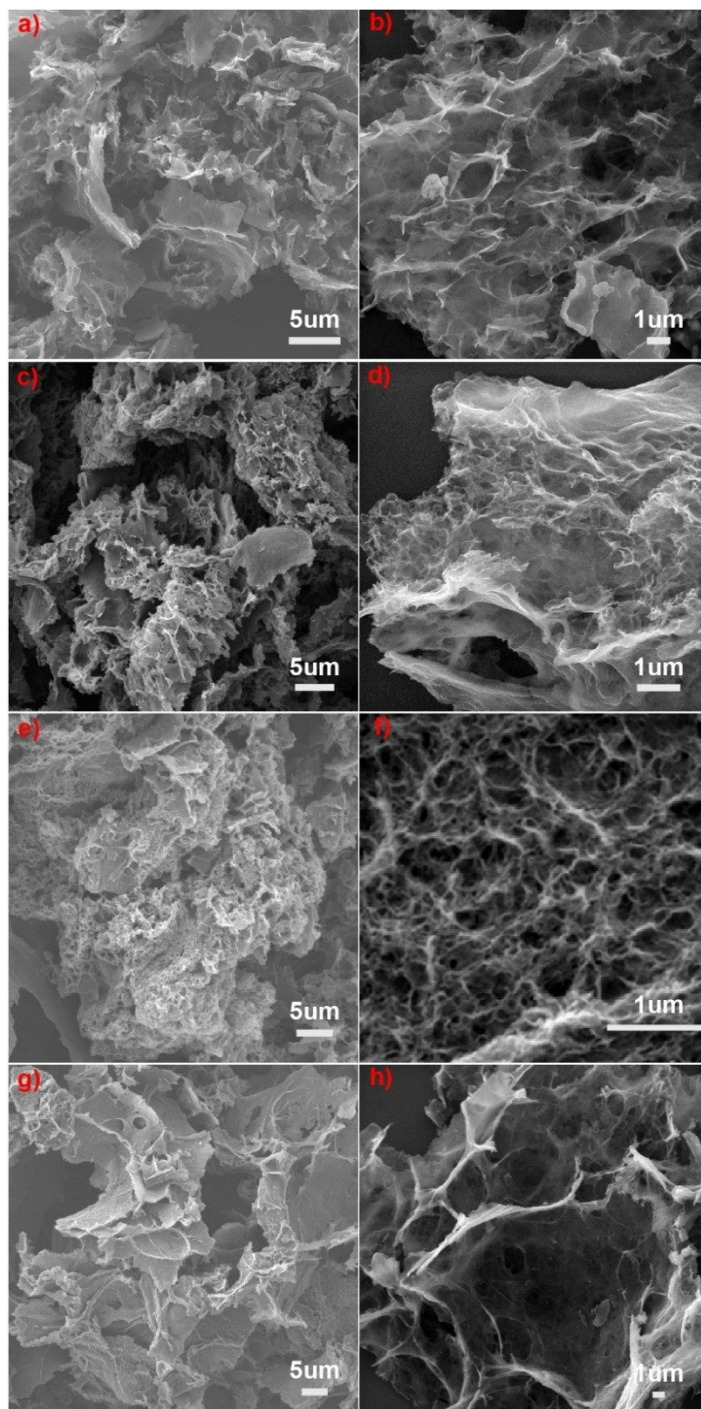


Fig. S5. SEM images of NGH-1(a, b); NGH-2(c, d); NGH-3(e, f); NGH-4(g, h);

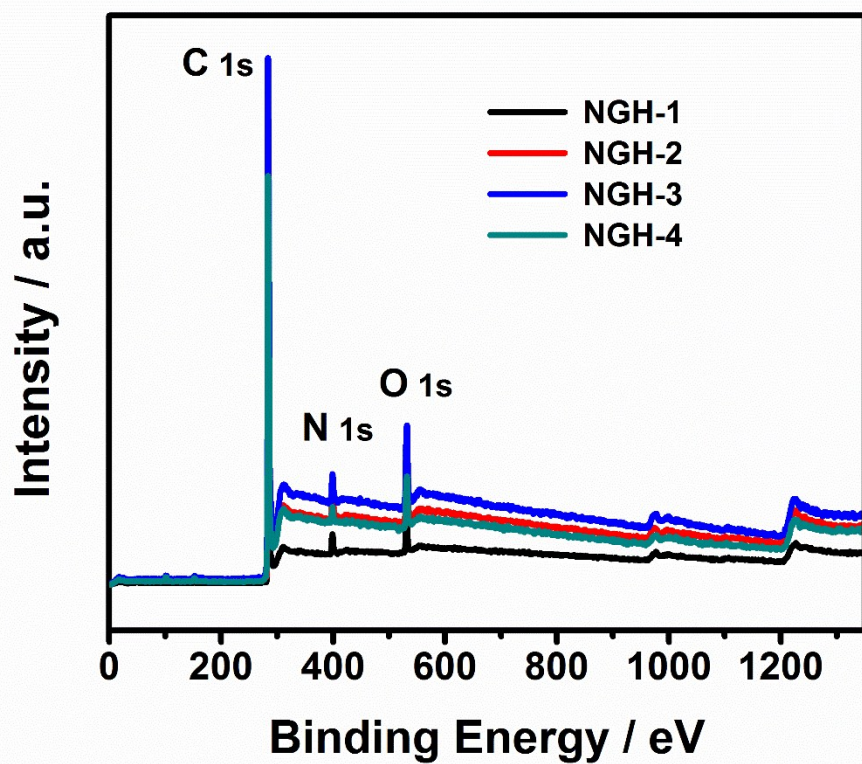


Fig. S6. XPS spectrum of NGHs.

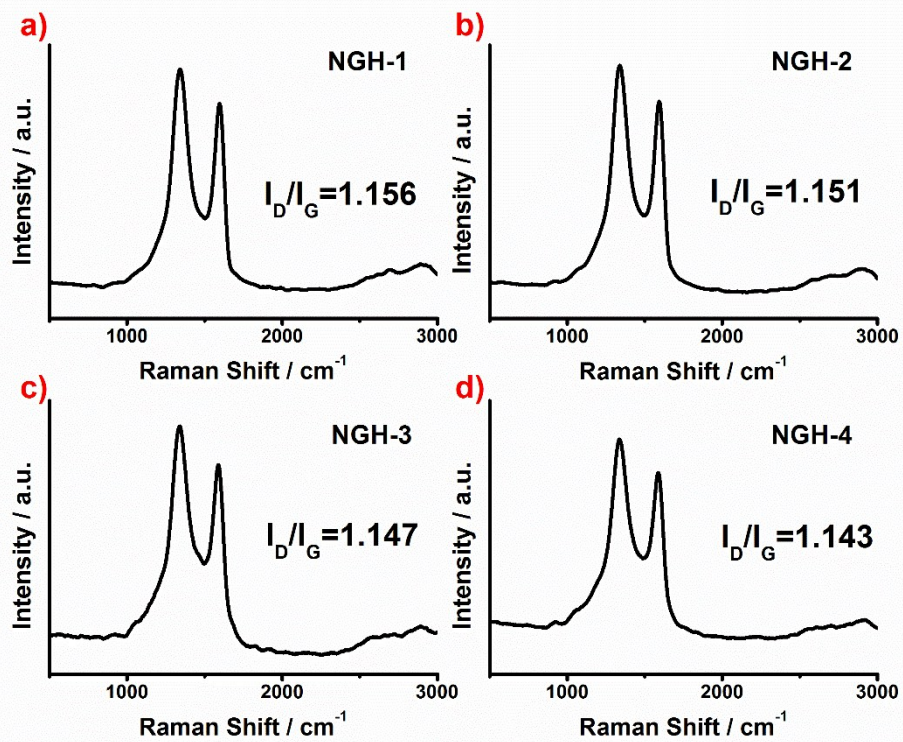


Fig. S7. Raman of NGH-1(a); NGH-2(b); NGH-1(c); NGH-1(d)



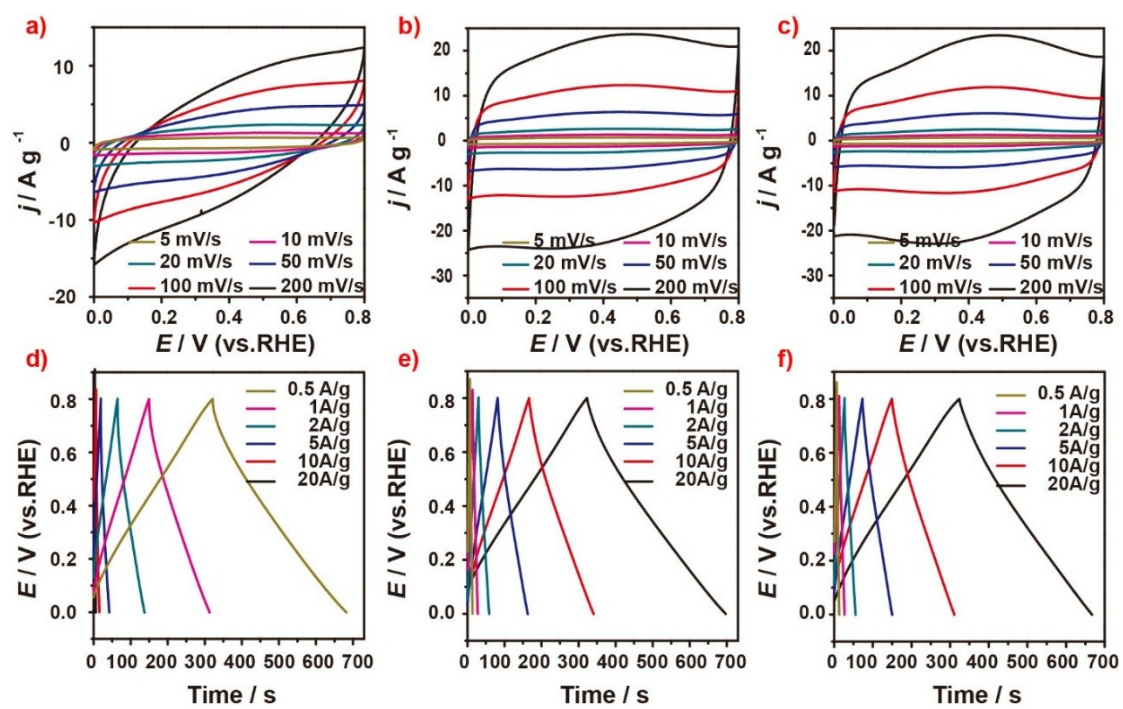


Fig. S8. (a, b, c) CV curves of NGHs for different scan rates. (d, e, f) Galvanostatic charge/discharge curves of NGHs under different constant currents. (a, d) NGH-1; (b, e) NGH-2; (c, f) NGH-4.

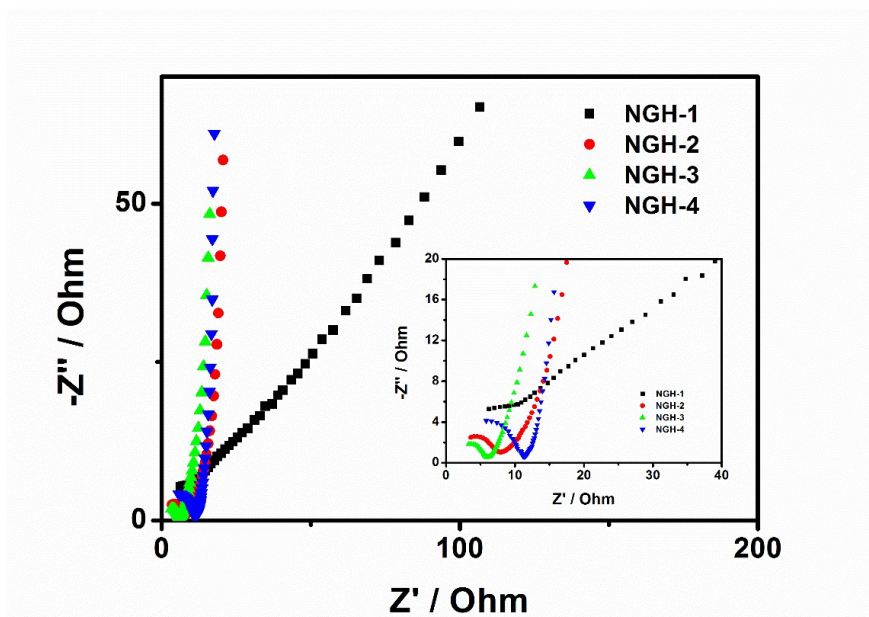


Fig. S9. Nyquist plots of the NGHs

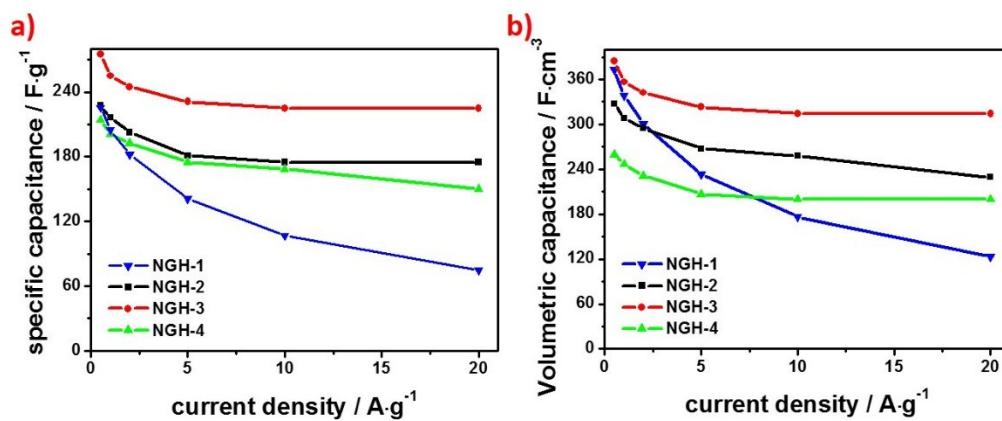


Fig. S10. The capacitance comparison of NGHs

Table. S1. The content of N.

	NGH-1	NGH-2	NGH-3	NGH-4
N	7.19 at.%	4.93 at.%	4.44 at.%	2.71%
Pyridinic N	32.72 at.%	27.17 at.%	26.28 at.%	25.40 at.%
Nitrile N	39.64 at.%	48.27 at.%	46.36 at.%	52.54 at.%
Quaternary N	27.62 at.%	16.16 at.%	14.55 at.%	10.62 at.%
Pyridinic-N-oxide	0	8.39 at.%	12.81 at.%	11.45 at.%

Table. S2. Comparison of NGH-3 with other graphene framework.

sample	method	capacitance	rate	system	Ref.
<b>This work</b>	Hydrothermal Process	275 F/g	0.5A/g	3	/
<b>self-assembled graphene hydrogel</b>	Hydrothermal Process	175F/g	1A/g	2	ACS Nano, 2010, 4(7), 4324–4330.
<b>graphene aerogel</b>	Sol–gel	128F/g	0.05A/g	2	J. Mater. Chem., 2011, 21, 6494–6497
<b>Graphene Hydrogels</b>	Hydrothermal Process	220F/g	1A/g	2	J. Phys. Chem. C 2011, 115, 17206–17212
<b>B,N-doped-GA</b>	Hydrothermal Process	239F/g	1mV/s	3	Adv. Mater. 2012, 24, 5130–5135
<b>N-doped-GA</b>		190F/g			
<b>B-doped-NG</b>		228F/g			
<b>Undoped-NG</b>		181F/g			
<b>Nitrogen-doped graphene sheets</b>	Hydrothermal Process	161F/g	0.5A/g	3	Electrochimica Acta, 2012, 85, 459-466.
<b>graphene aerogel - based mesoporous carbons</b>	Hydrothermal Process and calcination	226F/g	1mV/s	3	J. Am. Chem. Soc. 2012, 134, 19532–19535
		168F/g	2A/g		
<b>graphene aerogel</b>	Hydrothermal Process	176F/g	1mV/s		
<b>3D architectures of graphene</b>	Self-assembly	151.6F/g	0.5A/g	3	J. Mater. Chem., 2012, 22, 22459–22466
<b>nitrogen-doped graphene hydrogels</b>	Hydrothermal Process	190.1F/g	10A/g	2	Nano Energy, 2013, 2, 249–256
<b>nitrogen- and sulfur-codoped 3D mesoporous carbon</b>	calcination	320F/g	1A/g	3	ACS Appl. Mater. Interfaces, 2014, 6, 2657–2665
		143F/g	10A/g		
<b>Nitrogen-Doped Graphene</b>	Microwave Irradiation	200F/g	0.5A/g	3	ACS Appl. Mater. Interfaces, 2014, 6, 6361–6368
<b>RGO/CB</b>	vacuum filtration process	95.7F/g	0.5mV/s	2	Journal of Power Sources, 2014, 271, 269
<b>Nitrogen-Doped Graphene Aerogels</b>	Hydrothermal Process	176F/g	10A/g	2	ACS Appl. Mater. Interfaces 2015, 7, 1431–1438
		223F/g	0.2A/g		
<b>Crumpled</b>	Polymerization	245.9F/g	1A/g	2	Adv. Mater. 2012,

<b>Nitrogen-Doped Graphene</b>	and calcination	302F/g	5mV/s	3	24, 5610–5616
<b>HTrGO-B (ammonia solution treatment)</b>	Hydrothermal Process	185F/g	1A/g	2	Journal of Power Sources, 2013, 233, 313
<b>Activated Graphene</b>	Microwave Irradiation and KOH activation	165F/g	1.4A/g	2	Science 332, 1537–1541 (2011).
<b>Activated Reduced Graphene Oxide Films</b>	KOH activation	120F/g	10A/g	2	Nano Lett. 2012, 12, 1806–1812
<b>Activated Graphene based carbon</b>	Microwave Irradiation and KOH activation	172F/g	2A/g	2	ACS Nano, 2013, 7, 6899-6905
<b>nitrogen-doped graphene hydrogels</b>	Hydrothermal Process	246 F/g	3A/g	3	J. Mater. Chem. A, 2014, 2, 8352–8361
<b>3D hierarchical carbon</b>	sponge-templating with KOH activation	188F/g	1A/g	3	Adv. Mater. 2016, 28, 5222–5228
<b>3D porous carbon fabrics</b>	Hydrothermal Process	229 F/g	1A/g	3	ACS Appl. Mater. Interfaces 2015, 7, 4257–4264
<b>Reduced graphene oxide</b>	calcination	182 F/g	1A/g	2	Chem. Commun., 2015, 51, 5598-5601.
<b>3D Porous N-Doped Graphene</b>	Hydrothermal Process and calcination	509 F/g	1A/g	3	Adv. Mater. 2015, 27, 5171–5175
<b>Reduced graphene oxide</b>	using redox additive electrolyte	298F/g	0.8A/g	2	Carbon ,2015, 90, 260 –273
<b>Holey Graphene Oxide</b>	Hydrothermal Process and H <sub>2</sub> O <sub>2</sub> activation	283 F/g	1 A/g	3	Nano Lett. 2015, 15, 4605–4610
<b>Ultrathin porous carbon shell</b>	Calcination	251 F/g	1 A/g	3	Carbon, 2017, 111 419-427
<b>graphene nanoribbons</b>	Calcination and KOH	189 F/g	0.1A/g	2	Nature Chemistry, 2016, 8, 718–724

	activation				
<b>3D Graphene-like carbon</b>	Templating and calcination	252 F g	10mV/s	2	Carbon, 2017, 111 128-132